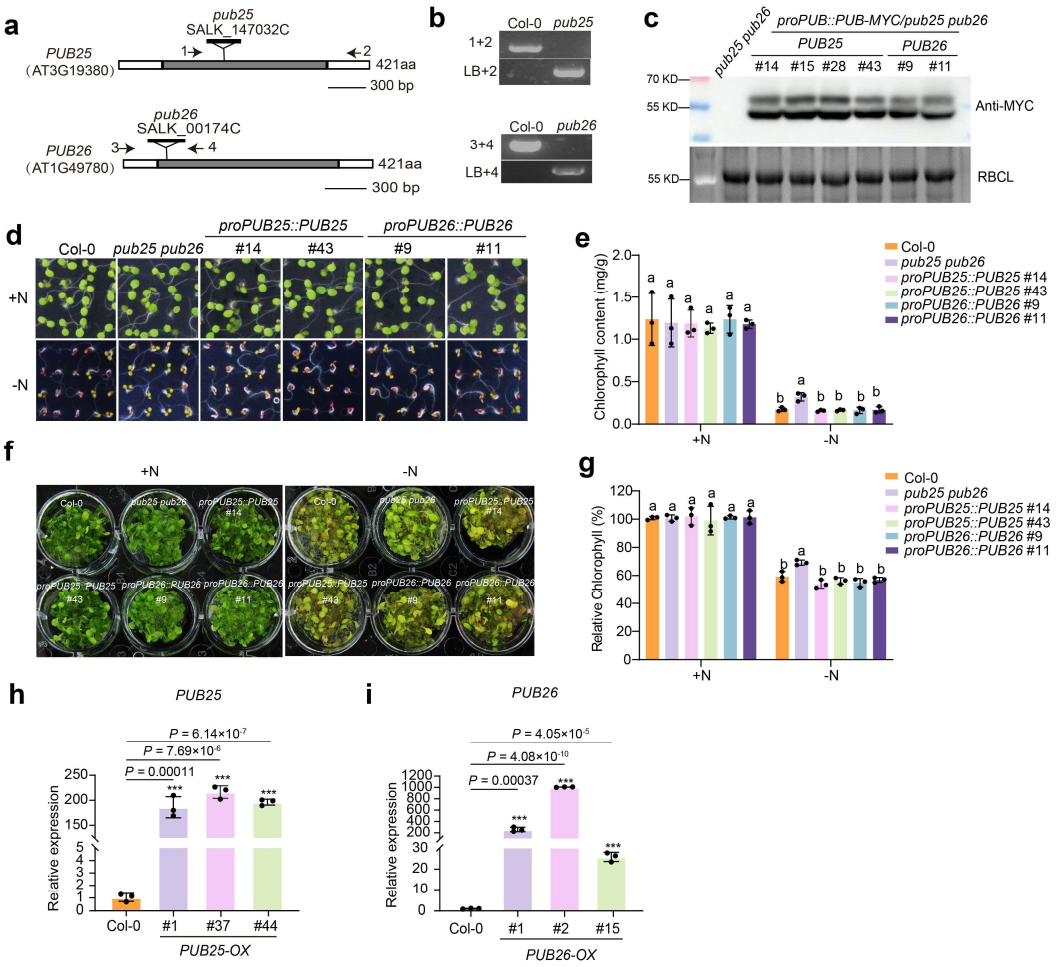

Supplementary Fig. 1 | Analysis of *pub25* and *pub26* single mutants, genetic complementation of *pub25 pub26* double mutant, and *PUB25/PUB26* overexpression lines.

a, b Genotyping of *pub25* and *pub26* single mutants. Arrows in (**a**) indicate primer positions; white and black boxes represent untranslated regions (UTRs) and exons, respectively. **c** PUB25 and PUB26 protein levels in complementation lines in the *pub25 pub26* double mutant background. Rubisco (RBCL) was used as a loading control. **d** Phenotypes of Col-0 and *pub25 pub26* complementation lines in response to nitrogen starvation. Seedlings were grown on +N or -N medium for 6 days. **e** Chlorophyll content of seedlings from (**d**). For each biological replicate, at least 64 plants were examined per genotype. Data are mean ± SD (n = 3). **f** Seedlings of the same genotypes as in (**d**) were pre-grown on +N medium for 7 days and then incubated in -N liquid

medium for 5 days. **g** Relative chlorophyll content of seedlings from (**f**), normalized to Col-0 under +N conditions (set to 100%). Data are mean ± SD (n = 3). For panels (**e, g**), statistical significance was determined by one-way ANOVA followed by Tukey's multiple comparison test ($P < 0.05$). Different letters denote significant differences. **h, i** Transcript levels of *PUB25* and *PUB26* in overexpression lines relative to Col-0. Data represent means ± SD (n = 3; ***$P < 0.001$, two-tailed unpaired Student's t-test).

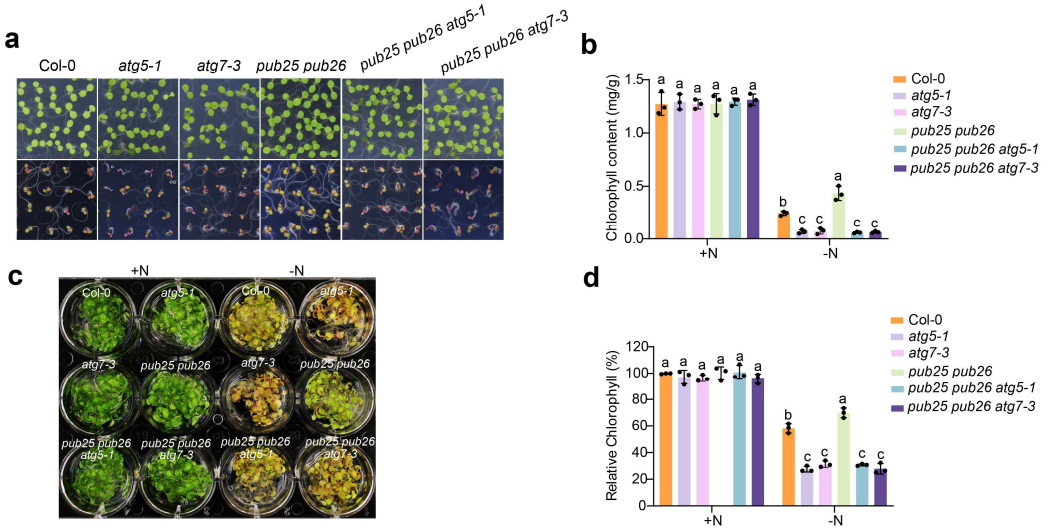

Supplementary Fig. 2 | Enhanced nitrogen starvation tolerance of *pub25 pub26* requires a functional autophagy pathway.

a Phenotypes of Col-0, *atg5-1*, *atg7-3*, *pub25 pub26*, *pub25 pub26 atg5-1*, and *pub25 pub26 atg7-3* triple mutants in response to nitrogen starvation. Seedlings were grown on +N or -N medium for 6 days. **b** Chlorophyll content of seedlings from (**a**). For each biological replicate, at least 64 plants were examined per genotype. Data are mean ± SD (n = 3). **c** Seedlings of the same genotypes as in (**a**) were pre-grown on +N medium for 7 days and then incubated in -N liquid medium for 5 days. **d** Relative chlorophyll content of seedlings from (**c**), normalized to Col-0 under +N conditions (set to 100%). Data are mean ± SD (n = 3). For panels (**b, d**), statistical significance was determined by one-way ANOVA followed by Tukey's multiple comparison test ($P < 0.05$).

Different letters denote significant differences.

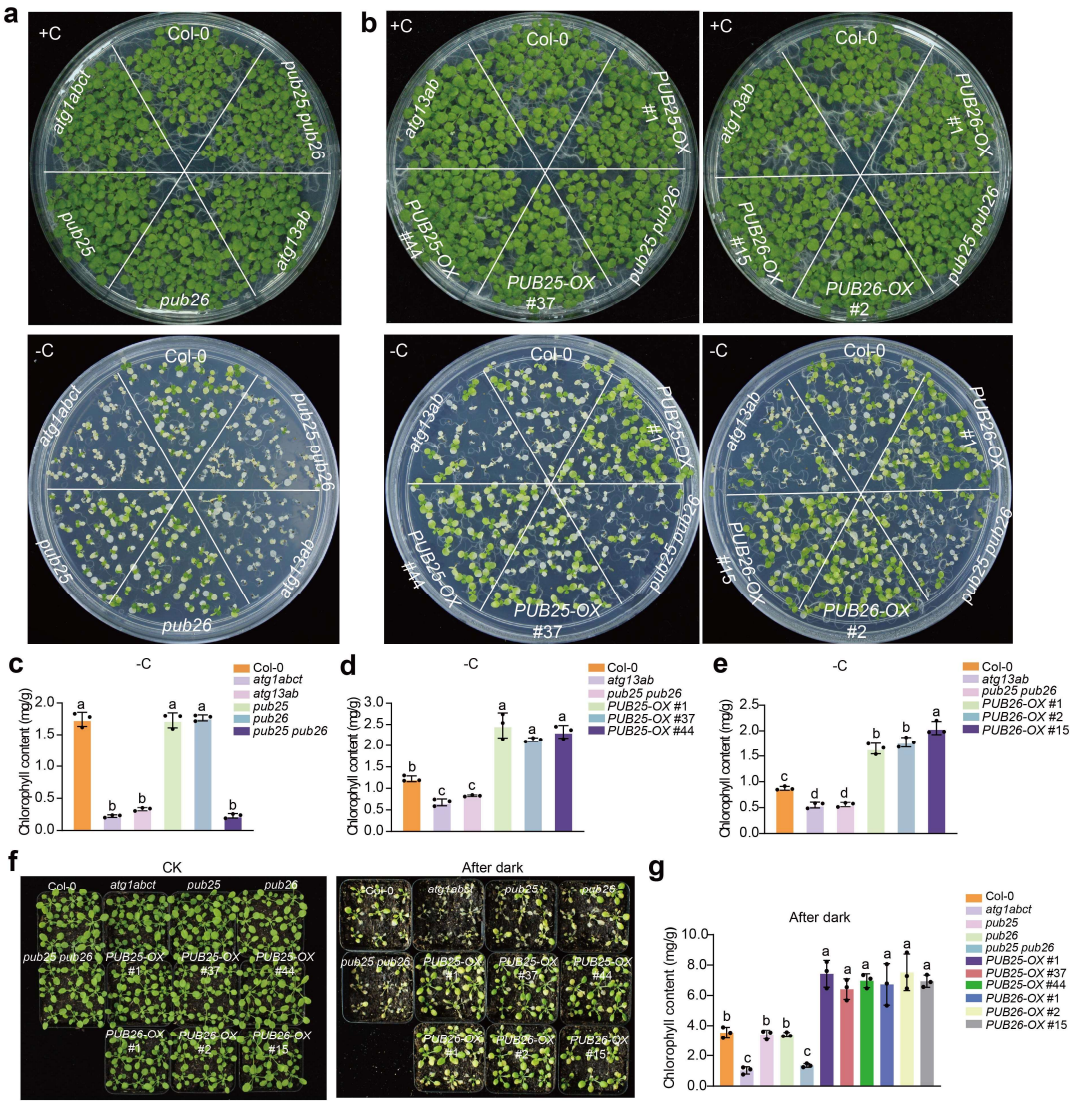

Supplementary Fig. 3 | PUB25 and PUB26 positively regulate plant tolerance to fixed-carbon starvation.

a, b Phenotypes of *pub25* and *pub26* single mutants, *pub25 pub26* double mutant, and *PUB25*- or *PUB26*-overexpression lines in response to fixed-carbon starvation. Seedlings were grown continuously on sucrose-containing 1/2 MS solid medium under long-day (LD; 16 h light/8 h dark) conditions (carbon-sufficient, +C), or on sucrose-free 1/2 MS solid medium under LD for 7 d, followed by 9-10 d of dark incubation and 3-4 d of recovery under LD (fixed-carbon-starved, -C). **c, d, e** Chlorophyll contents of seedlings in (**a**) and (**b**). For each biological replicate, at least 25 plants were examined

per genotype. Data are mean ± SD (n = 3). **f** Phenotypes of 3-week-old *pub25* and *pub26* single mutants, *pub25 pub26* double mutant, and *PUB25*- or *PUB26*-overexpression lines before and after 7 d of dark incubation. **g** Chlorophyll contents of seedlings in **(f)**. For each biological replicate, at least 8 plants were examined per genotype. Data are mean ± SD (n = 3). For panels (**c, d, e, g**), statistical significance was determined by one-way ANOVA followed by Tukey's multiple comparison test ($P < 0.05$). Different letters denote significant differences.

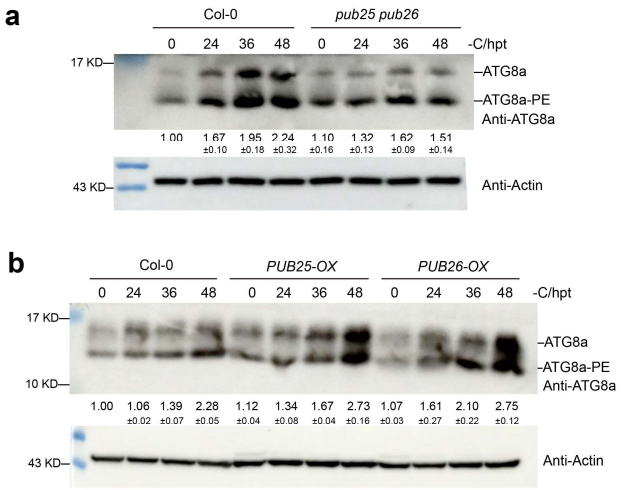

Supplementary Fig. 4 | ATG8a lipidation levels in Col-0, *pub25 pub26* double mutant, and *PUB25*- or *PUB26*-overexpressing lines under fixed-carbon starvation.

a ATG8a lipidation in Col-0 and *pub25 pub26* double mutant in response to fixed-carbon starvation. **b** ATG8a lipidation in Col-0 and *PUB25*- or *PUB26*-overexpressing lines upon fixed-carbon starvation. ATG8a-PE levels (normalized to actin) are indicated below lanes in (**a, b**). Data represent mean ± SD (n = 3). hpt, hours post-treatment.

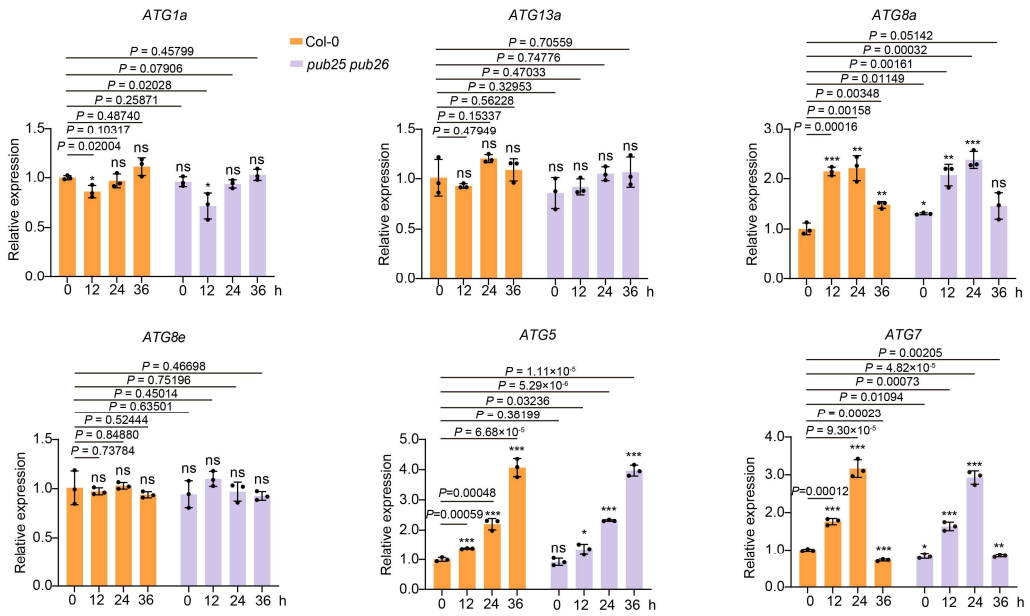

Supplementary Fig. 5 | Expression of autophagy-related genes (*ATGs*) in Col-0 and *pub25 pub26* double mutant under nitrogen starvation. Seven-day-old Col-0 and *pub25 pub26* double mutant seedlings were subjected to nitrogen starvation for 0, 12, 24, or 36 h prior to RNA extraction. *Ubiquitin 10 (UBQ10*) was used as the internal control. Expression levels were normalized to Col-0 at 0 h (set to 1). Data represent mean ± SD ($n = 3$). Asterisks indicate statistically significant differences compared with Col-0 at 0 h (two-tailed unpaired Student's *t*-test, $*P < 0.05$; $**P < 0.01$; $***P < 0.001$).

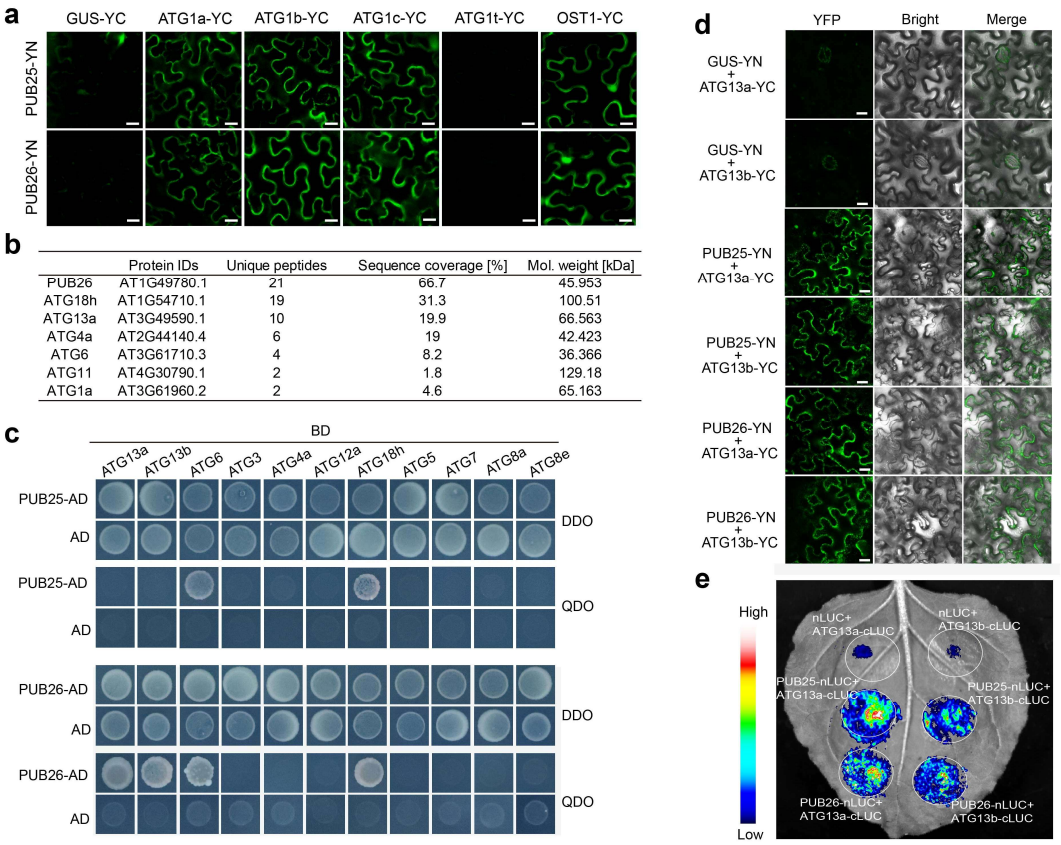

Supplementary Fig. 6 | PUB25 and PUB26 interact with other ATGs.

a Bimolecular fluorescence complementation (BiFC) assays **s**howing that PUB25 and PUB26 interact with ATG1s in *N. benthamiana*. Scale bars, 10 μm. β-glucuronidase (GUS) and OST1 were used as the negative and positive controls, respectively. **b** Screening for PUB26-interacting autophagy-related proteins by immunoprecipitation-mass spectrometry (IP-MS) analysis. Total proteins were extracted from *proPUB26::PUB26-MYC/pub25 pub26* seedlings, immunoprecipitated with anti-MYC beads, and subjected to in-gel digestion followed by LC-MS/MS analysis. **c** Interaction of PUB25 and PUB26 with autophagy-related proteins in Y2H assays. **d** BiFC assays showing that PUB25 and PUB26 interact with ATG13s in *N. benthamiana*. Scale bars, 10 μm. **e** Split-LUC assays reveal that PUB25 and PUB26 interact with ATG13s.

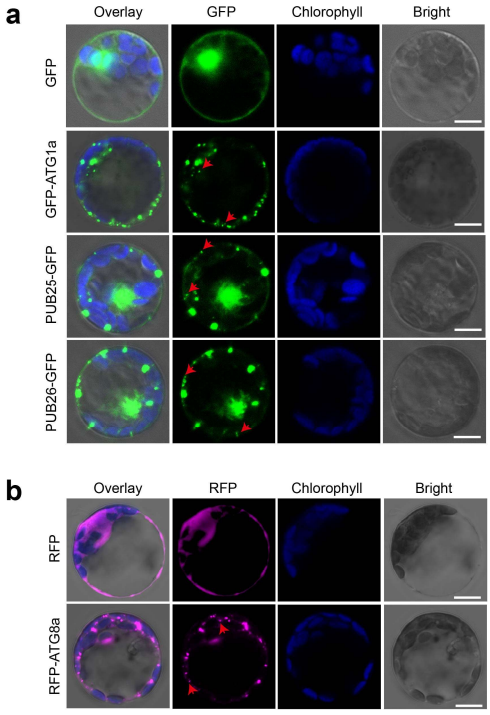

Supplementary Fig. 7 | Subcellular localization of PUB25, PUB26, ATG1a, and ATG8a in Arabidopsis protoplasts.

a Transient expression of PUB25-GFP, PUB26-GFP, or GFP-ATG1a in Arabidopsis protoplasts. Transformed protoplasts were incubated at 22°C in darkness for 16 h. Free GFP was used as a negative control. Red arrows indicate punctate structures resembling autophagosomes labeled with PUB25-GFP, PUB26-GFP, or GFP-ATG1a. Scale bars, 10 μm. **b** Subcellular localization of RFP-ATG8a in Arabidopsis protoplasts. Free RFP was used as a negative control. Red arrows indicate autophagosomes labeled with RFP-ATG8a. Scale bars, 10 μm.

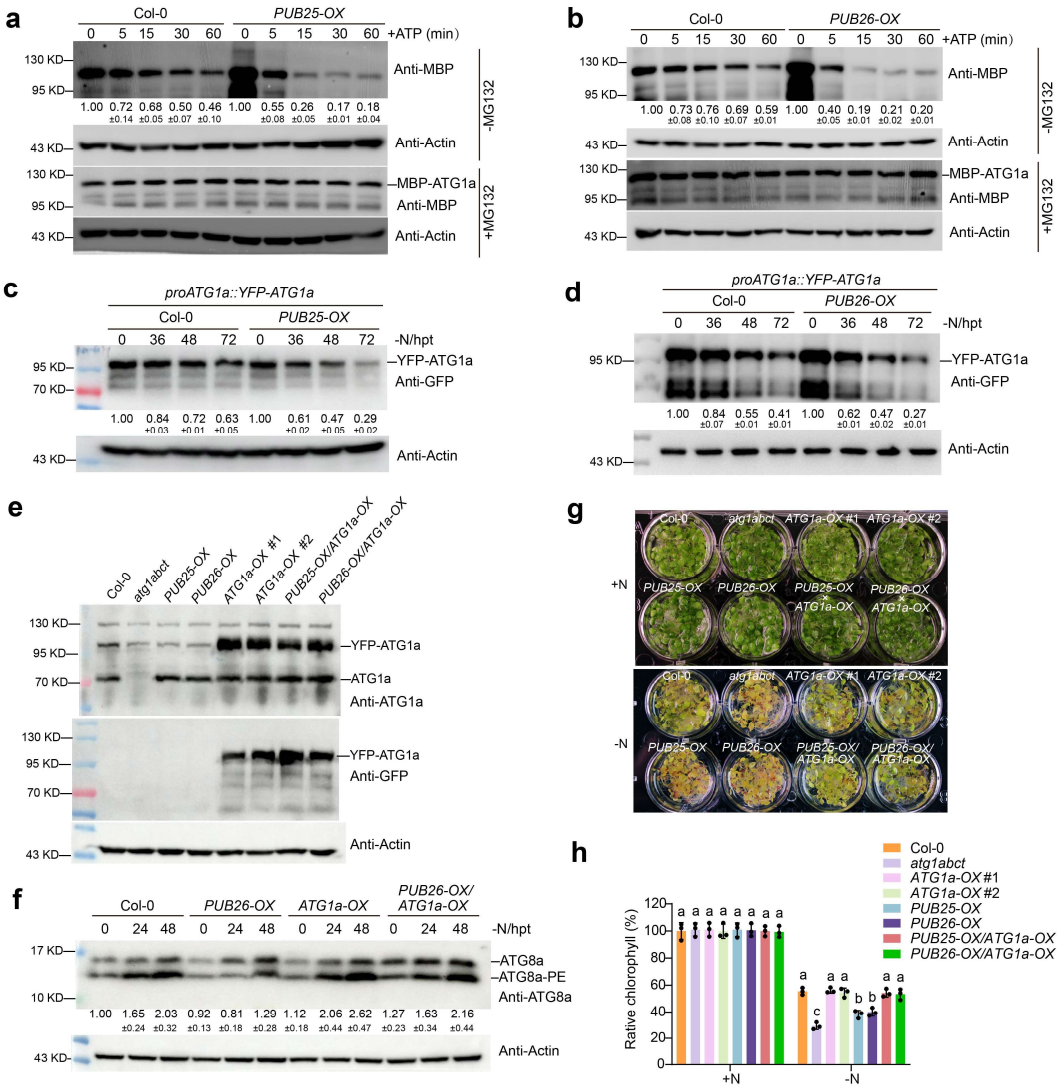

Supplementary Fig. 8 | PUB25 and PUB26 negatively regulate ATG1a protein stability.

a, b PUB25 and PUB26 promotes ATG1a degradation in cell-free assay. Recombinant MBP-ATG1a was incubated with total protein extracts from Col-0 or *PUB25*- or *PUB26*-overexpression seedlings with or without 5 μM MG132, and detected by anti-MBP antibody. Values below lanes indicate MBP-ATG1a levels normalized to actin. Data represent mean ± SD ($n = 3$). **c, d** YFP-ATG1a protein levels in Col-0 and *PUB25*- or *PUB26*-overexpressing lines under nitrogen starvation. Values below lanes indicate YFP-ATG1a levels normalized to actin. Data represent mean ± SD ($n = 3$). **e** Immunoblot analysis of ATG1a protein levels in Col-0, *atg1abct* quadruple mutant, and

transgenic plants expressing 35S::PUB25-FLAG, 35S::PUB26-FLAG, 35S::YFP-ATG1a, or 35S::YFP-ATG1a together with 35S::PUB25-FLAG and 35S::PUB26-FLAG. **f** Introduction of 35S::YFP-ATG1a into the *PUB25*- or *PUB26*-overexpressing lines restores nitrogen starvation induced autophagy. ATG8a-PE levels (normalized to actin) are indicated below the lanes. Data represent mean ± SD (n = 3). **g** Introduction of 35S::YFP-ATG1a into the *PUB25- or PUB26*-overexpressing lines restores nitrogen starvation tolerance. **h** Relative chlorophyll content of seedlings from (**g**), normalized to Col-0 under +N conditions (set to 100%). Data are mean ± SD (n = 3; one-way ANOVA with Tukey's multiple comparison test, $P < 0.05$).

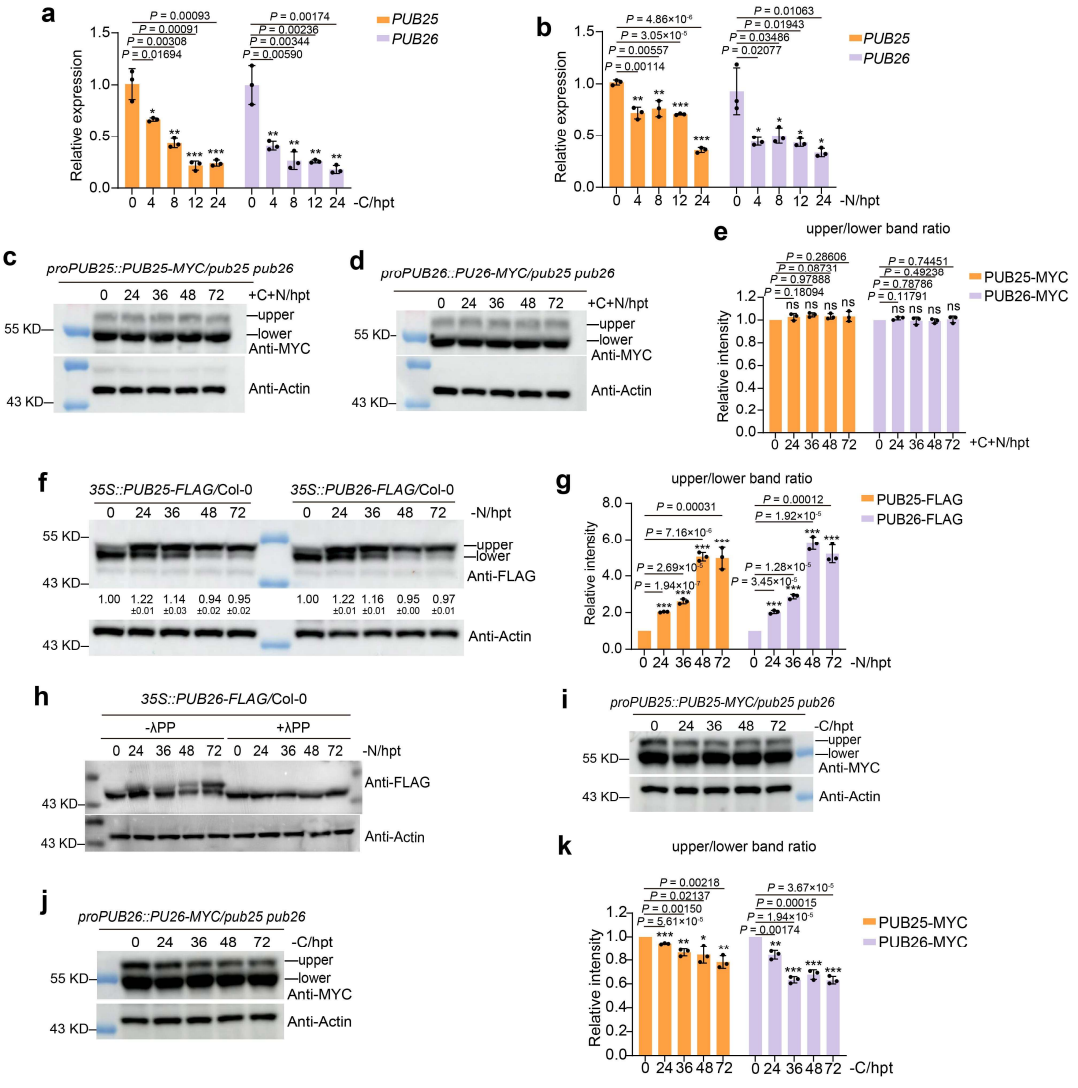

Supplementary Fig. 9 | Nitrogen starvation triggers phosphorylation of PUB25

and PUB26.

a, b Transcript levels of *PUB25* (**a**) and *PUB26* (**b**) under fixed-carbon starvation and nitrogen starvation. Data represent mean ± SD (n = 3). Asterisks indicate statistically significant differences compared with 0 h (two-tailed unpaired Student's t-test, *P < 0.05; **P < 0.01; ***P < 0.001). **c, d** Mobility shift assays of PUB25-MYC (**c**) and PUB26-MYC (**d**) under normal (nutrient-sufficient) conditions. **e** Quantification of the phosphorylated (upper) versus non-phosphorylated (lower) PUB-MYC ratio from (**c, d**). Data are mean ± SD (n = 3, two-tailed unpaired Student's t-test). **f** Immunoblot analysis of PUB25-FLAG and PUB26-FLAG under nitrogen starvation. Col-0 stably expressing 35S::PUB25-FLAG or 35S::PUB26-FLAG were subjected to nitrogen starvation; total protein extracts were immunoblotted with anti-FLAG antibody. Numbers below lanes indicate total protein levels of PUB-FLAG normalized to actin (mean ± SD, n = 3). **g** Quantification of the phosphorylated (upper) versus non-phosphorylated (lower) PUB-FLAG ratio from (**f**). Data are mean ± SD (n = 3, ***P < 0.001, two-tailed unpaired Student's t-test). **h** λ-Phosphatase (λPP) treatment confirms that the mobility shift in (**f**) is due to phosphorylation. **i, j** Mobility shift analysis of PUB25-MYC (**i**) and PUB26-MYC (**j**) under fixed-carbon starvation. **k** Quantification of the phosphorylated (upper) versus non-phosphorylated (lower) PUB-MYC ratio from (**i, j**). Data are mean ± SD (n = 3, *P < 0.05; **P < 0.01; ***P < 0.001, two-tailed unpaired Student's t-test).

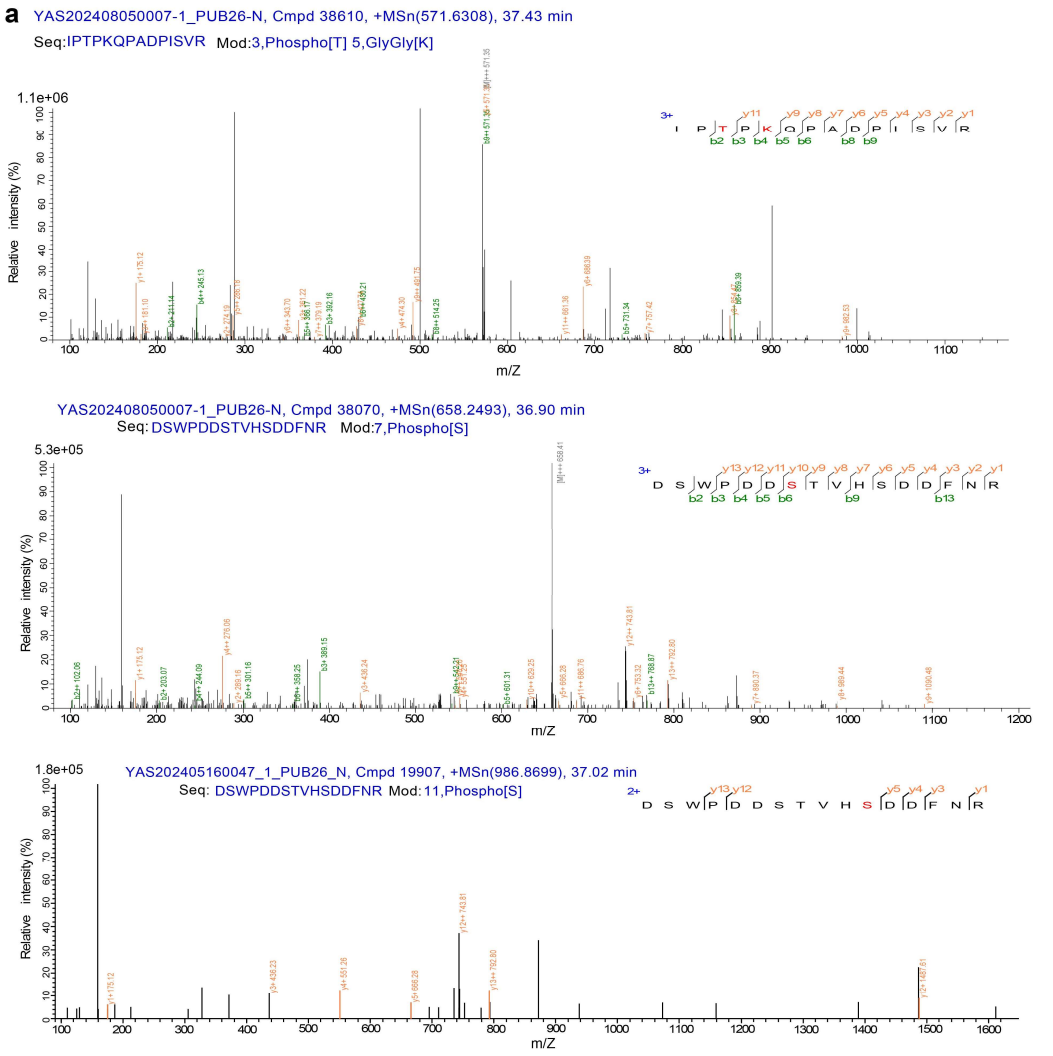

b

Proteins	Phospho (STY) Probabilities	Intensity PUB26+N	Intensity PUB26-N	Positions
AT1G49780.1	IPT(1)PKQPADPISVR	8706600	24412000	T94
AT1G49780.1	DSWPDDS(0.598)T(0.155)VHS(0.247)DDFNR	0	35767000	S406
AT1G49780.1	DS(0.001)WPDDS(0.009)T(0.009)VHS(0.981)DDFNR	15288000	53248000	S410

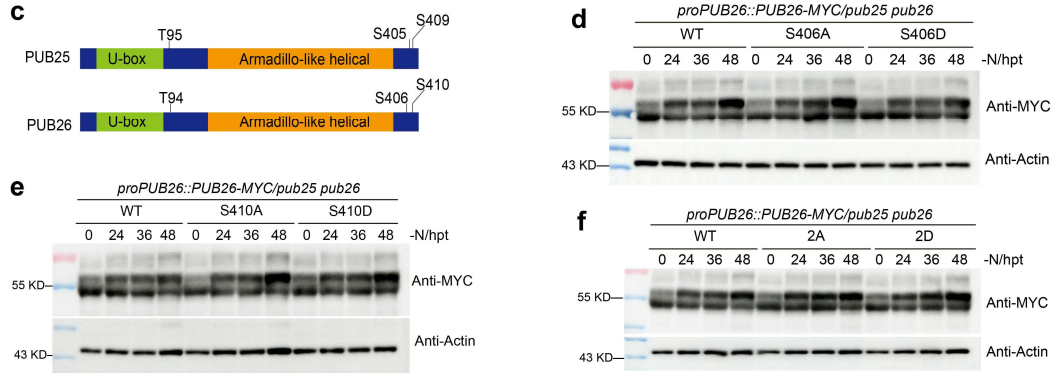

Supplementary Fig. 10 | Effects of Ser406 and Ser410 mutations on nitrogen starvation-induced PUB26 phosphorylation.

a, b IP-MS analysis of phosphorylated PUB26 peptides under nitrogen starvation. Seedlings of *proPUB26::PUB26-MYC/pub25 pub26* were subjected to nitrogen starvation prior to immunoprecipitation with anti-MYC beads. Affinity-purified proteins were subjected to LC-MS/MS analysis. **c** Schematic diagram showing the identified phosphorylation sites in PUB26 and the corresponding conserved residues in PUB25. **d, e, f** Effects of Ser406 and Ser410 mutations on nitrogen starvation-induced PUB26 phosphorylation. The *pub25 pub26* double mutant expressing PUB26-MYC variants with single-site mutations (S406A/S406D/S410A/S410D) or combined mutations (2A, S406A/S410A; 2D, S406D/S410D) driven by PUB26 native promoter were subjected to nitrogen starvation for various durations. Total proteins were extracted and immunodetected using anti-MYC antibody. hpt, hours post-treatment.

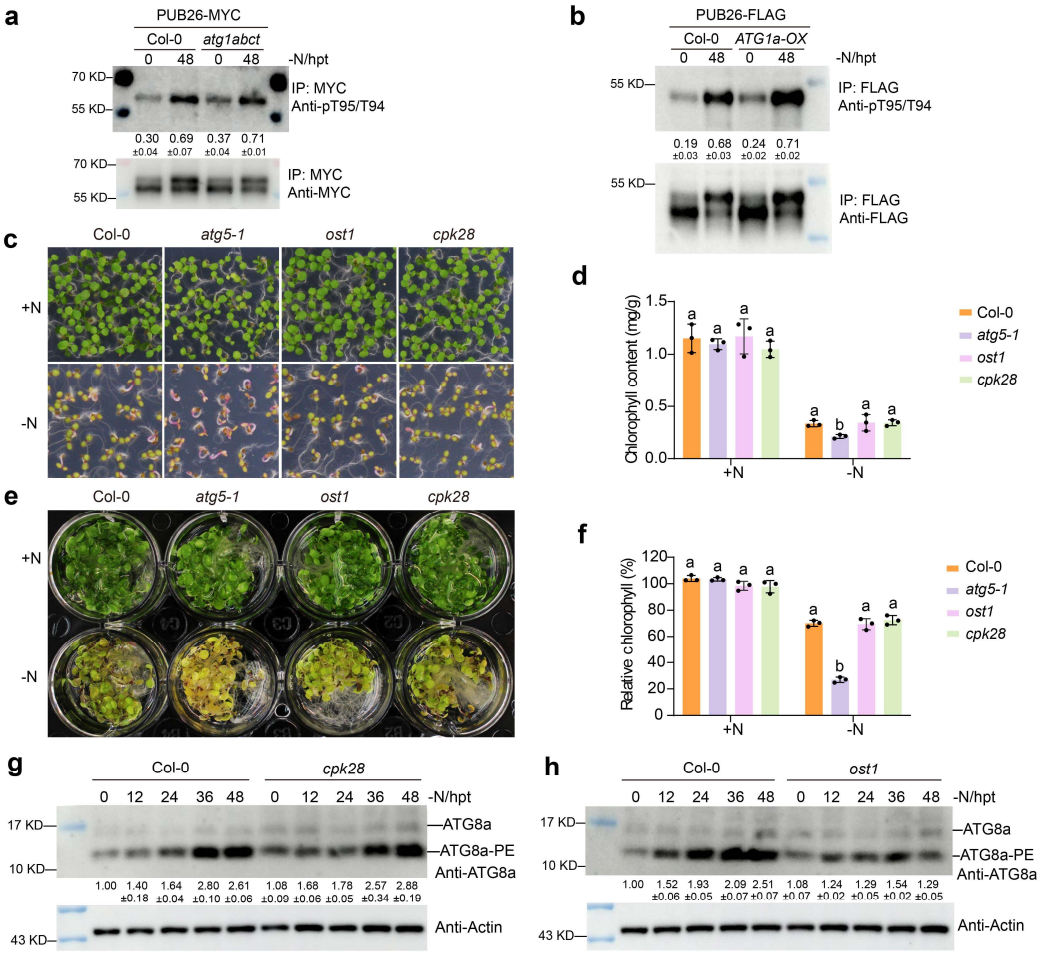

Supplementary Fig. 11 | Effect of ATG1 kinase on nitrogen starvation-induced

phosphorylation of PUB26 at Thr94, and nitrogen starvation-induced autophagy in *ost1* and *cpk28* mutants.

a, b Thr94 phosphorylation of PUB26 in Col-0, *atg1abct* mutant, and *ATG1a* overexpression lines under nitrogen starvation. Transgenic plants expressing 35S::PUB26-MYC (**a**) or 35S::PUB26-FLAG (**b**) were subjected to nitrogen starvation. Proteins were immunoprecipitated with anti-MYC beads (**a**) or anti-FLAG beads (**b**) and probed with anti-pT95/T94 antibody. Values below lanes indicate the relative Thr94 phosphorylation signal normalized to immunoprecipitated PUB26-MYC or PUB26-FLAG levels. Data are mean ± SD (n = 3). **c** Phenotypes of Col-0, *ost1*, and *cpk28* mutants in response to nitrogen starvation. Seedlings were grown on +N or -N medium for 6 days. **d** Chlorophyll content of seedlings from (**c**). For each biological replicate, at least 64 plants were examined per genotype. **e** Phenotypes of the same genotypes as in (**c**) after transfer to -N liquid medium. Seedlings were pre-grown on +N medium for 7 days and then incubated in -N liquid medium for 5 days. **f** Relative chlorophyll content of seedlings from (**e**), normalized to Col-0 under +N conditions (set to 100%). For (**d**, **f**), data are mean ± SD (n = 3), one-way ANOVA with Tukey's multiple comparison test ($P < 0.05$). **g, h** Immunoblot analysis of ATG8a lipidation in Col-0, *ost1*, and *cpk28* under nitrogen starvation. ATG8a-PE levels (normalized to actin) are indicated below the lanes. Data are mean ± SD (n = 3).

a

Protein IDs	Description	Unique peptides PUB26+N	Unique peptides PUB26-N	Sequence coverage PUB26+N [%]	Sequence coverage PUB26-N [%]
AT1G49780.1	PUB26	23	21	83.8	81.7
AT5G21326.1	CIPK26	9	3	25.1	9.1
AT4G23650.1	CPK3	9	8	23.4	20.8
AT3G29160.2	KIN11	9	7	18.2	14.2
AT4G33950.2	OST1	5	6	13.1	16.2
AT2G17290.2	CPK6	4	4	6.2	6.2
AT3G51550.1	FERONIA	5	8	6	9.6
AT1G50030.2	TOR	9	9	5.4	5.4
AT1G60490.1	ATVPS34	1	5	1.4	7.2
AT4G08850.1	MIK2	0	7	0	8.2
AT2G31880.1	SOBIR1	0	2	0	3.4

b

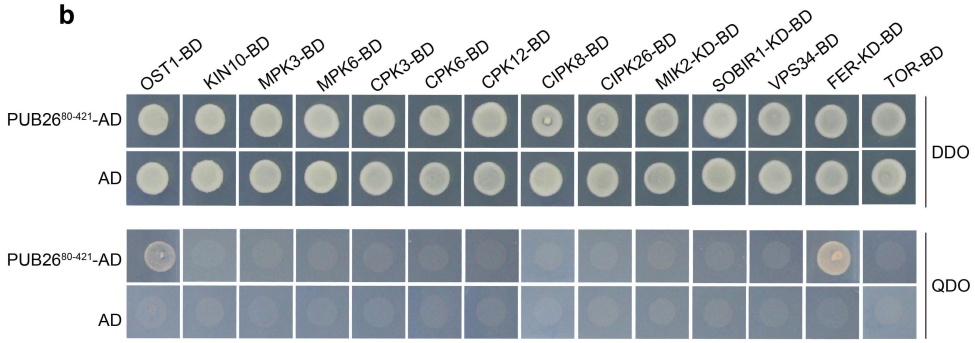

Supplementary Fig. 12 | Screen for kinases potentially interacting with PUB26.

a IP-MS analysis to screen for kinases potentially interacting with PUB26 under +N or –N conditions. Transgenic plants *proPUB26::PUB26-MYC/pub25 pub26* were subjected to N-rich and N-starvation treatments, total proteins were extracted, followed by immunoprecipitation with anti-MYC-beads, and the products were analyzed by LC-MS/MS. **b** Y2H assay showing interactions between truncated PUB26 (PUB26$^{80-421}$) and various kinases. For transmembrane receptors MIK2, SOBIR1, and FERONIA, their intracellular kinase domains (KDs) were used for the interaction assay. OST1 was used as a positive control.

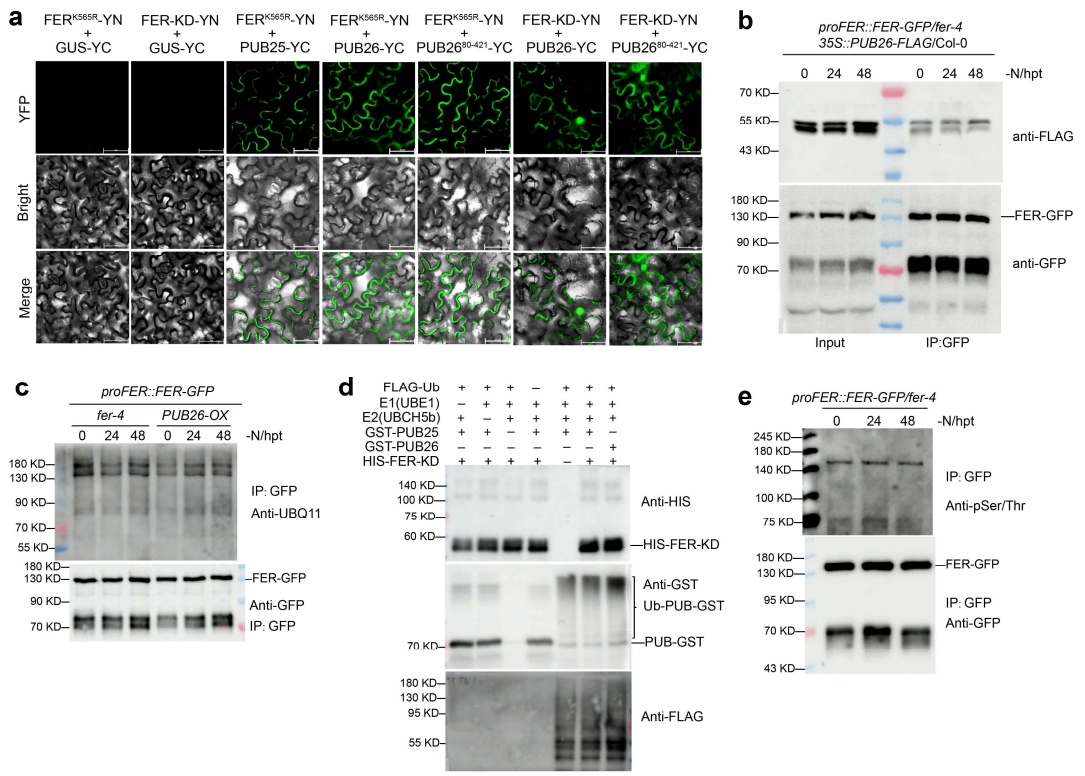

Supplementary Fig. 13 | FERONIA interacts with PUB25 and PUB26, and is not ubiquitinated by PUB25 or PUB26.

a BiFC assays confirm interactions between PUB25 and PUB26 (or their truncated versions) and either the full-length kinase-dead variant FER^{K565R} (wild-type FER induces severe cell death in transiently transformed *N. benthamiana* leaf cells, so the kinase-dead K565R mutant was used instead) or the truncated FER-KD. GUS-YC served as a negative control. Scale bars = 50 μm. **b** Co-IP assay to detect the interaction between PUB26 and FER under nitrogen starvation conditions. Total proteins were extracted from Arabidopsis lines co-expressing FER-GFP and PUB26-FLAG following nitrogen starvation for the indicated times. hpt, hours post-treatment. **c** Ubiquitination levels of FER in *fer-4* and *PUB26-OX* backgrounds under nitrogen starvation. Total protein extracts were isolated from nitrogen-starved *proFER::FER-GFP/fer-4* and *proFER::FER-GFP/PUB26-OX* seedlings, followed by immunoprecipitation with anti-GFP beads, and detected by anti-UBQ11 antibody. **d** In vitro ubiquitination assay of the

FER kinase domain (FER-KD) by PUB25 and PUB26. Reaction mixtures were incubated with 10 mM ATP at 37°C for 5 h. Ubiquitination was detected with the indicated antibodies. **e** Immunoblot analysis of FER phosphorylation under nitrogen starvation. Total protein extracts were isolated from nitrogen-starved *proFER::FER-GFP/fer-4* seedlings, followed by immunoprecipitation with anti-GFP beads and detected via immunoblotting using anti-pSer/Thr antibody.

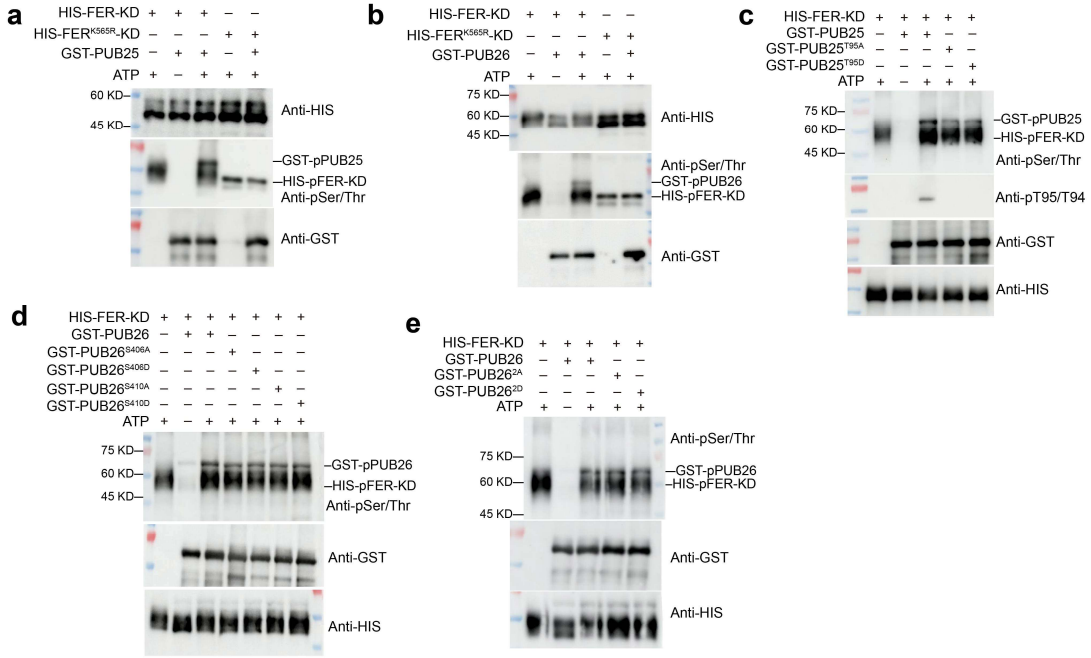

Supplementary Fig. 14 | FERONIA phosphorylates PUB25 and PUB26 in vitro.

a, b In vitro phosphorylation of PUB25 and PUB26 by FER-KD and kinase-dead FER^{K565R}-KD. Recombinant proteins were incubated in phosphorylation reaction buffer containing 1 mM ATP at 30°C for 30 min. Phosphorylated proteins were detected by anti-pSer/Thr antibody. **c** In vitro phosphorylation of PUB25 Thr94 variants by FER-KD. Phosphorylated proteins were detected by anti-pSer/Thr antibody and anti-pT95/T94 antibody. **d, e** In vitro phosphorylation of PUB26 Ser406/Ser410 variants by FER-KD. Phosphorylated proteins were detected by anti-pSer/Thr antibody. 2A (S406A/S410A), 2D (S406D/S410D).

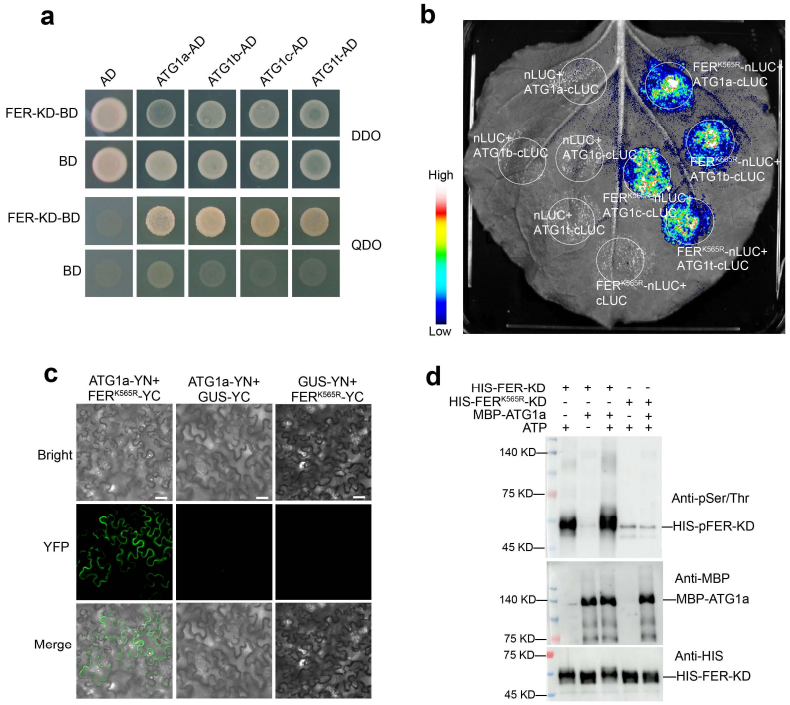

Supplementary Fig. 15 | FERONIA interacts with but does not phosphorylate ATG1.

a Y2H assay showing interactions between the FER kinase domain (FER-KD) and ATG1s (ATG1a, ATG1b, ATG1c). **b** Split-LUC assays confirm interactions between the FER functional variant FER^{K565R} and ATG1s. **c** BiFC assays of the interactions between the FER functional variants FER^{K565R} and ATG1a. GUS-YN and GUS-YC served as negative controls. Scale bars = 10 μm. **d** In vitro phosphorylation of ATG1a by FER-KD and kinase-dead FER^{K565R}-KD. Phosphorylated proteins were detected by anti-pSer/Thr antibody.

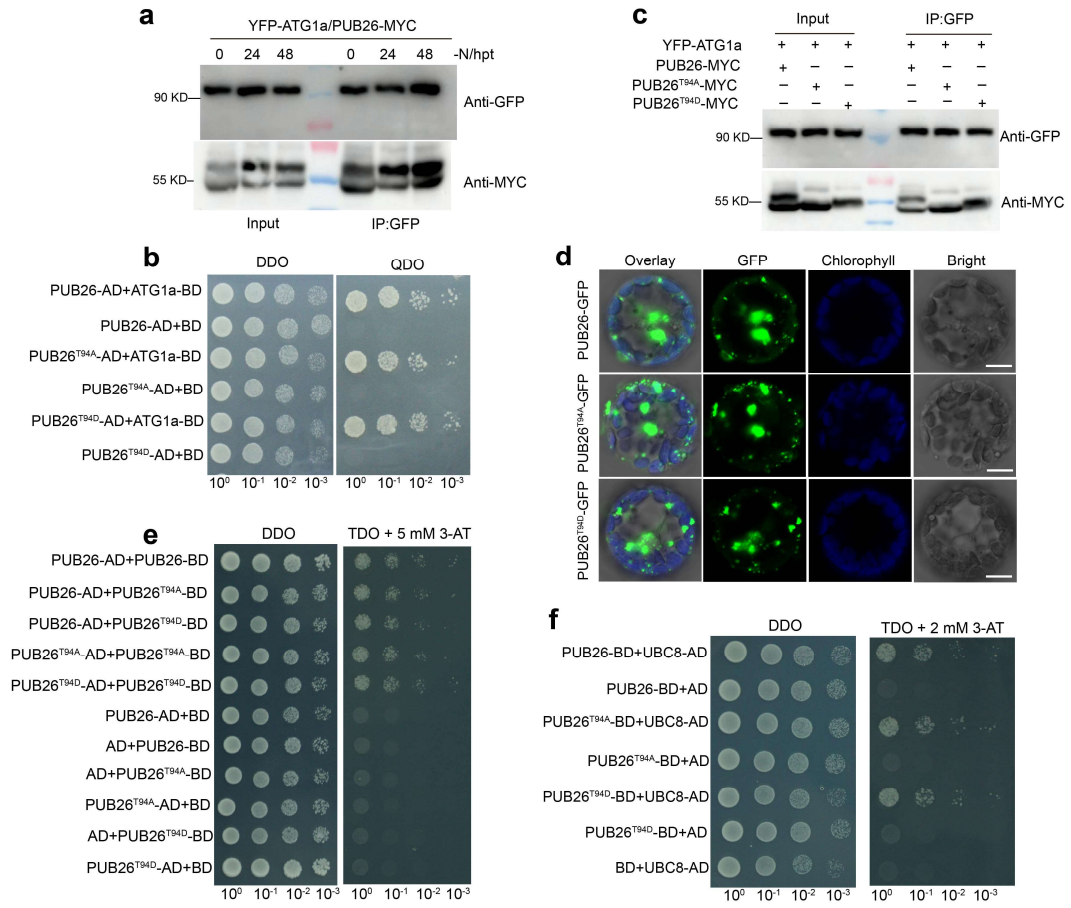

Supplementary Fig. 16 | Effects of PUB26 phosphorylation on its interaction with substrate ATG1a, subcellular localization, dimerization, and interaction with the E2 enzyme (UBC8).

a Co-IP assay to detect the interaction between PUB26 and ATG1a under nitrogen starvation conditions. Total proteins were extracted from transgenic plant co-expressing YFP-ATG1a and PUB26-MYC following nitrogen starvation for the indicated times. hpt, hours post-treatment. **b** Y2H assay to detect the interaction between ATG1a and PUB26 variants (wild-type, T94A, and T94D). **c** Co-IP assay of PUB26 variants (wild-type, T94A, and T94D) with ATG1a. Total proteins were extracted from Arabidopsis co-expressing PUB26-MYC, PUB26^{T94A}-MYC or PUB26^{T94D}-MYC with YFP-ATG1a following nitrogen starvation. hpt, hours post-treatment. **d** Subcellular localization of PUB26 Thr94 variants in protoplasts isolated from *pub25 pub26* double mutant. Scale

bars, 10 μm. **e** Y2H assay to analyze the effect of Thr94 phosphorylation on PUB26 dimerization using PUB26 variants (WT, T94A, T94D). **f** Y2H assay to analyze the effect of Thr94 phosphorylation on PUB26-UBC8 interaction using PUB26 variants (WT, T94A, T94D).

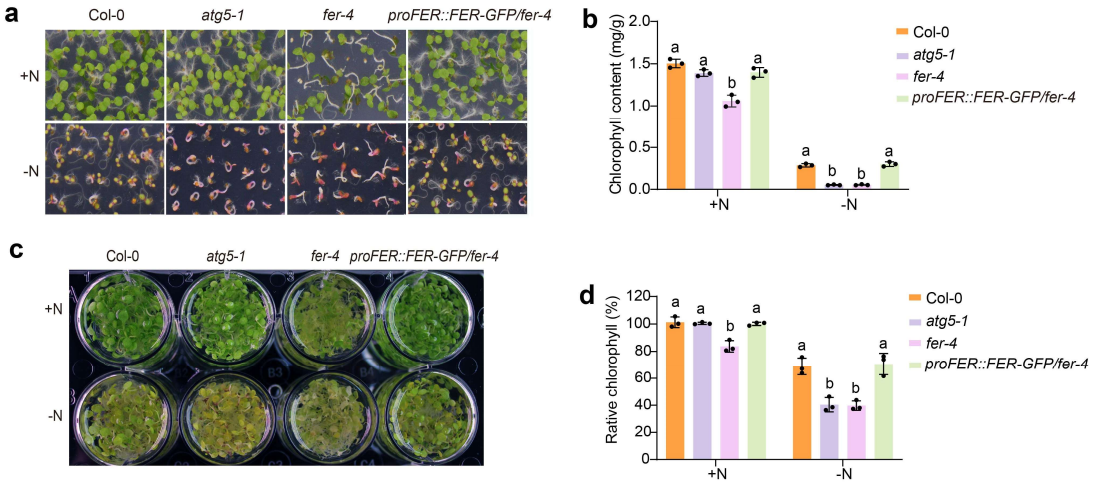

Supplementary Fig. 17 | Loss of FER function confers hypersensitivity to nitrogen starvation in plants.

a Phenotypes of Col-0, *atg5-1*, *fer-4*, and *proFER::FER-GFP/fer-4* seedlings in response to nitrogen starvation. Seedlings were grown on +N or -N medium for 6 days. **b** Chlorophyll content of seedlings from (**a**). Data are mean ± SD (n = 3). For each biological replicate, at least 64 plants were examined per genotype. **c** Phenotypes of the same genotypes as in (**a**) after transfer to -N liquid medium. Seedlings were pre-grown on +N medium for 7 days and then incubated in -N liquid medium for 3 days. **d** Relative chlorophyll content of seedlings from (**c**), normalized to Col-0 under +N conditions (set to 100%). Data are mean ± SD (n = 3). For (**b, d**), statistical significance was determined by one-way ANOVA followed by Tukey's multiple comparison test (P < 0.05).

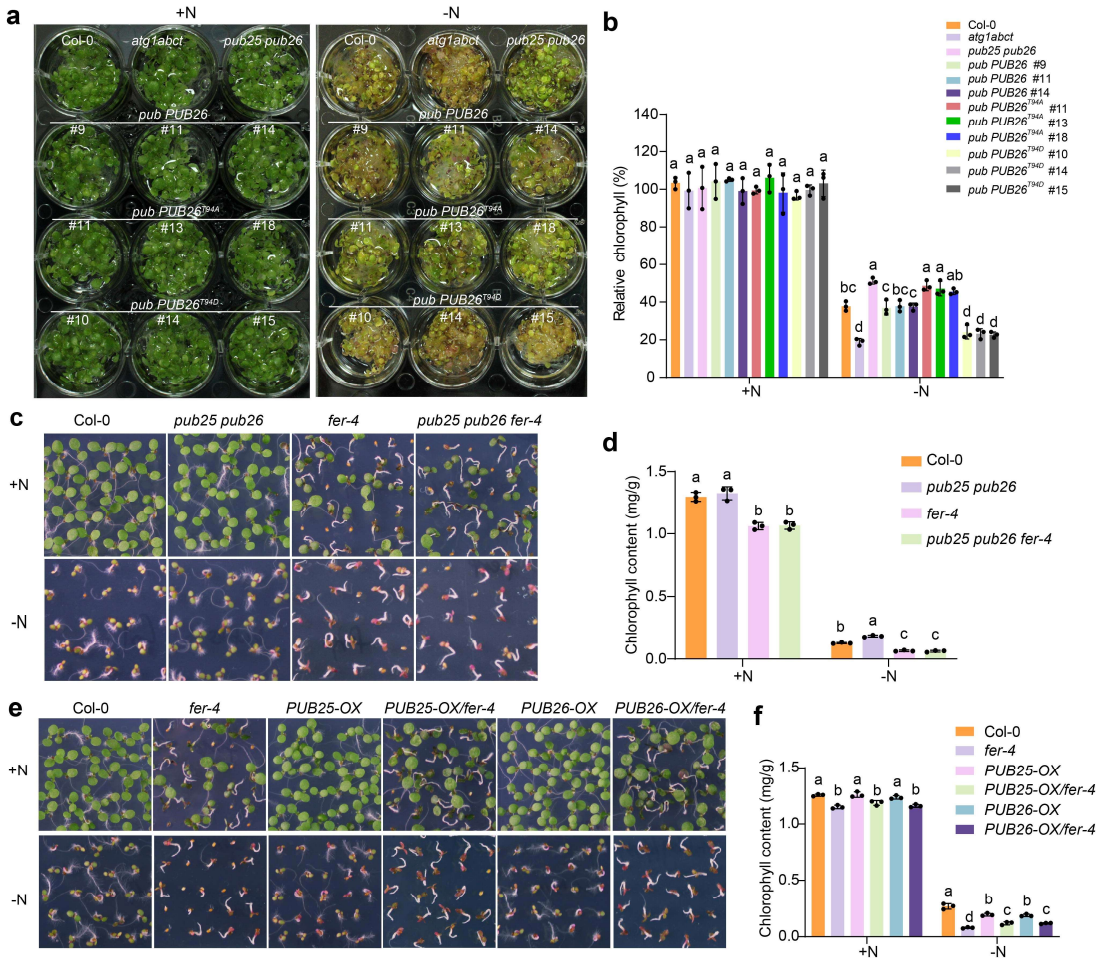

Supplementary Fig. 18 | FERONIA-mediated phosphorylation of PUB26 negatively regulates nitrogen starvation-induced plant autophagy.

a PUB26 Thr94 phosphorylation enhances plant sensitivity to nitrogen starvation. Seedlings of the indicated genotypes pre-grown on +N medium for 7 days and then incubated in -N liquid medium for 5 days. **b** Relative chlorophyll content of seedlings from (**a**), normalized to Col-0 under +N conditions (set to 100%). Data are mean ± SD (n = 3). **c** Phenotypes of Col-0, *pub25 pub26*, *fer-4* and *pub25 pub26 fer-4* triple mutant under nitrogen starvation. Seedlings were grown on +N or -N medium for 6 days. **d** Chlorophyll content of seedlings from (**c**). Data are mean ± SD (n = 3). For each biological replicate, at least 64 plants were examined per genotype. **e** Phenotypes of Col-0, *fer-4*, *PUB25-OX*, *PUB26-OX*, *PUB25-OX/fer-4*, and *PUB26-OX/fer-4* plants under nitrogen starvation. **f** Chlorophyll content of seedlings from (**e**). Data are mean ±

SD (n = 3). For (**b, d, f**), statistical significance was determined by one-way ANOVA followed by Tukey's multiple comparison test ($P < 0.05$).

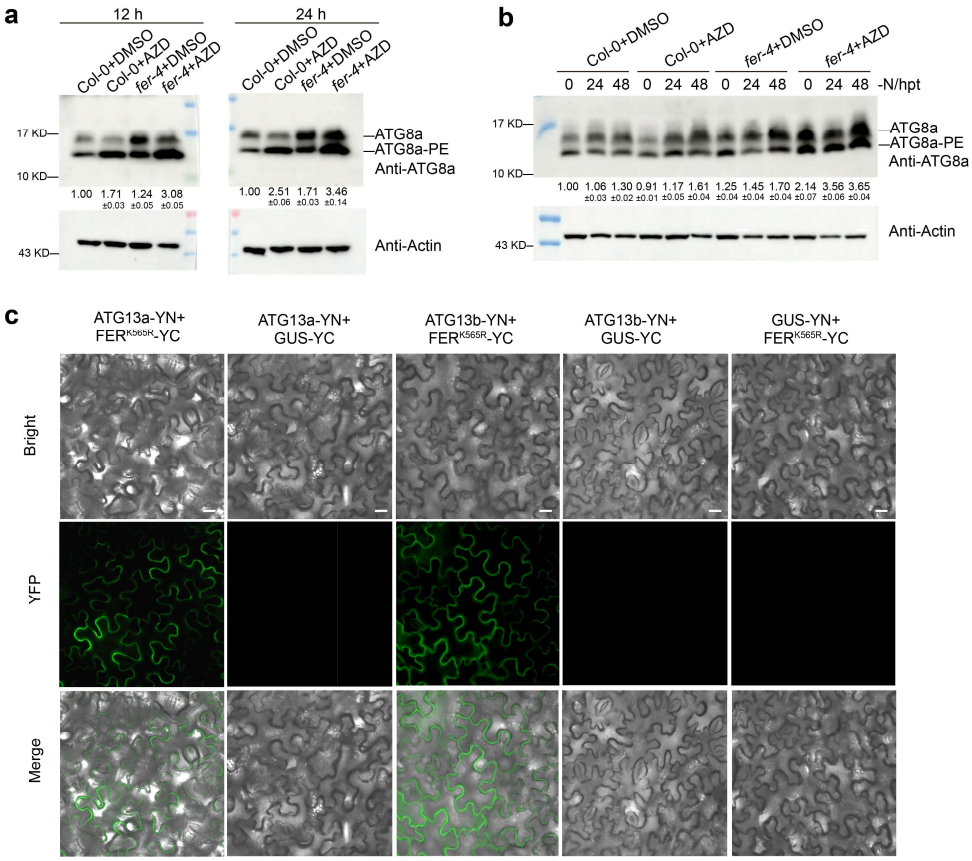

Supplementary Fig. 19 | FER suppresses autophagy through partially TOR-independent pathways, and FER interacts with ATG13.

a, b AZD8055 treatment enhances ATG8a lipidation in the *fer-4* mutant. Total proteins were extracted from Col-0 and *fer-4* seedlings treated with DMSO or AZD8055 (1 μM), and analyzed by anti-ATG8a antibody. ATG8a-PE levels normalized to actin are shown below lanes. Data are mean ± SD (n = 3). **c** BiFC assays of the interactions between the FER functional variants FER^{K565R} and ATG13. GUS-YN and GUS-YC served as negative controls. Scale bars = 10 μm.